Secure Mobile Edge Computing via a Drone-enabled FSO-based Heterogeneous Network

Weiqi Liu, Graduate Student member, IEEE, Shuai Zhang, Member, IEEE, and Nirwan Ansari, Fellow, IEEE

Abstract—A secure mobile edge computing (MEC) framework, which leverages free space optics (FSO) to provision backhauling from drone-mounted base stations (DBSs) to a macro base station (MBS), is proposed. DBSs can work as computing nodes to provide computing services to user equipments (UEs) as well as relays to forward the tasks to the MBS at the same time. Both DBSs and MBS are provisioned with servers. UEs can offload their tasks to the MBS directly, DBSs directly, or the MBS via a DBS. The DBSs are to be placed at the optimal locations to provide computing services and uplink communications for the ground UEs. We then formulate the joinT bandwidth and computation rEsource assignment, DBS traNsmisSion power contrOl, UE power contRol, UE association and DBS placement (TENSOR) problem to jointly maximize the average secrecy rate and minimize the task completion time. Since TENSOR is a mixed-integer nonlinear problem, we decompose it into four subproblems: resource (bandwidth and computation) assignment and DBS transmission power control problem, UE power control problem, UE association problem, and DBS placement problem. Successive convex approximation and an iterative algorithm are leveraged to solve the four sub-problems separately. In each iteration, we use the output of the first three as the input for the fourth. The performance of our algorithm is superior to the greedy algorithm, block search placement algorithm, and equally shared resource allocation algorithm upon which the average secrecy rate is improved by at least 19%.

Index Terms—drone-mounted base station (DBS), edge computing, resource allocation, FSO, security

I. INTRODUCTION

With the deployment of 5G networks and the proliferation of mobile devices, a myriad of applications such as mixed reality, natural language processing, face recognition, and health monitoring are emerging. These advanced applications are usually computationally intensive and time-sensitive, and impose great challenges to be executed on mobile devices [1]. By leveraging Mobile Cloud Computing (MCC), mobile devices can offload their tasks to remote cloud servers. However, the total number of connected devices in the world in 2025 is estimated to be over 41.2 billion including 30.9 billion IoT devices and 5.8 billion mobile phones [2]; offloading tasks to the remote servers may incur long transmission time and congestions. Deploying drone-mounted base stations (DBSs) can empower 5G and beyond networks with additional flexibility. DBSs can bring the computing resources closer to the mobile devices, thus relieving the burden of the clouds [3]; they also likely

This work was supported in part by National Science Foundation under Grant CNS-1814748.

Weiqi Liu, Shuai Zhang and Nirwan Ansari are with the Advanced Networking Laboratory, Department of Electrical and Computing Engineering, New Jersey Institute of Technology, Newark, NJ 07102 USA (e-mails: {wl296, sz355, nirwan.ansari}@njit.edu).

provide line-of-sight (LoS) connections to mobile devices, thus potentially reducing the path loss and increasing the transmission rates. DBSs are typically resources-limited as compared to macro base stations (MBSs) [4]. When the number of mobile devices under the coverage of a DBS is large, the DBS may not be able to handle all the tasks. To alleviate this problem, the DBS can forward the computationally intensive tasks to MBS [5]. However, the backhaul link may suffer from high path loss when the DBS flies far away from the MBS to serve cell edge users. As a result, the transmission rate is significantly reduced. To overcome the issue, FSO can be leveraged to potentially provision high capacity. With broad spectrum bandwidth and small divergence angle, an FSO link can achieve a data rate of 1-2 Gbps over distances in the range of 1-5 km [6] - [8]. In addition, the FSO link will not cause interference to the access link since it is working on the unlicensed spectrum which does not overlap with the existing spectrum.

Despite the advantages of the DBS-assisted network, the information can be vulnerable to attacks due to the physical broadcast property of the wireless communication channels. With the increasing demand for broadcast services such as wireless local area networks and uplink communication in the cellular networks, the concern about broadcasting confidential messages is growing. The security issue is even more severe in MEC networks since all UEs can offload their data to the MEC servers (e.g., the user's personal information may be exposed to the eavesdropper when uploading a figure containing some private information to the server for image processing). As a result, the security has become an essential issue for the 5G and beyond networks. Physical layer security techniques can be employed to protect wireless communications. Different from the key-based encryption protocols implemented in the network, transport, session, and application layers, physical layer security techniques can protect the legitimate transmission without using the complex protocols and pre-shared keys in securing the DBS-assisted networks.

II. STATE OF THE ARTS

A wide range of research related to DBS-assisted networks has been studied. Al-Hourani *et al.* [9] studied LoS and non-LoS air to ground communications and proposed a probabilistic model to closely approximate the air to ground communication model recommended by the International Telecommunication Union. They also calculated the optimal altitude for a DBS to obtain the maximum coverage. Zhang and Ansari [10] proposed DBS-aided MEC architecture to provision communication and computing services for IoT devices.

A $(1+\epsilon)$ -approximation algorithm was proposed to minimize the operation cost of the whole network. Yang et al. [11] constructed a multi-DBS-aided mobile edge computing system to assist IoT networks. A differential evolution-based multi-UAV deployment mechanism was proposed to balance the task load in the network. A deep reinforcement learning algorithm was conceived for task scheduling in the DBSs. Si et al. [12] studied the communication system when both active and passive eavesdroppers exist in the network and proposed to implement cooperative jamming against the eavesdroppers. They proposed a new zero-forcing beamforming scheme to optimize the transmission power allocation between the information signal and artificial noise signal to maximize the achievable secrecy rate. Yao and Ansari [13] studied the application of fog-aided internet of drones for federated learning, where the training data are collected by the DBS and analyzed in the fog node. They proposed to control the transmission power of the DBS to maximize the secrecy rate of the federated learning system. A low complexity algorithm was proposed to obtain the optimal secrecy rate. Liu et al. [14] investigated the full-duplex active eavesdropper in a network scenario with a ground user sending signals to a DBS and simultaneously sending artificial noise to jam an eavesdropper. The hybrid security outage probability is derived and the optimal power allocation between the signal and the artificial noise as well as the DBS height is determined to minimize the hybrid security outage probability. Zhao et al. [33] studied hyper-dense smallcell networks and proposed to deploy UAVs to reduce the pressure of wireless backhaul. A cooperation scheme between the UAV and BS, where the UAV can functionally replace the BS and the idle BS can generate jamming signals to disrupt eavesdropping, is proposed. Jamming signals are designed to degrade the eavesdropper's channel. Cheng et al. [16] investigated UAV-relayed wireless networks and proposed a novel scheme where the UAV first finds two UEs which have mutually cached the files that were requested by the other, and then broadcasts the files requested by both UEs so that the eavesdropper does not know which file is requested by which UE. The secrecy rates of the non-cached UEs are maximized by optimizing the trajectory of the UAV and the UE association. Miao and Zeng [17] investigated the DBSenabled mobile relay system and proposed to implement jammer UAV against the eavesdropper on the ground. The maximum achievable secrecy rate is obtained by optimizing the trajectory and the transmit power of both the relay DBS and the jammer DBS.

Different from the above works, the motivation of this work is to maximize the achievable secrecy rate and minimize the task completion time in the MEC network at the same time. In our work, we do not introduce artificial noise (AN) because AN, though can jam the eavesdroppers, does corrupt the wireless channel, thus degrading the transmission rate of the devices in the network. Owing to the mobility of the DBS, we try to maximize the secrecy rate of all offloading users by optimizing the DBS placement, the transmission power of the user equipment (UEs), and UE association. The minimum task completion time is achieved by optimizing the DBS placement, the transmission power of UEs, UE association,

bandwidth, and computing resource allocation. To achieve the objective, we formulate the join<u>T</u> bandwidth and computation r<u>E</u>source assignment, DBS tra<u>N</u>smis<u>S</u>ion power cont<u>P</u>Ol, UE power cont<u>P</u>Ol, UE association and DBS placement (TENSOR) problem, and jointly maximize the average secrecy rate and minimize the task completion time.

The main contributions of this article are delineated as follows:

- An FSO-based DBS-assisted secure MEC framework is proposed where the laser is implemented as the backhaul from the DBSs to the MBS. DBSs can work as computing nodes to provide computing services for UEs as well as relays to forward the tasks to the MBS at the same time.
- 2) A cooperative framework between the DBSs and UEs is proposed to maximize the secrecy rate of all the offloading UEs by optimizing the DBSs placement, UE transmission power, and UE association.
- 3) A multi-hop, multi-choice, and multi-objective problem is formulated to maximize the secrecy rate and minimize task completion time of all offloading UEs. An iterative algorithm is proposed to solve the TENSOR problem.

The remainder of this article is organized as follows. Section III describes the up link communication models (including UE to DBS and UE to MBS). The task computing model is presented. The problem formulation is elucidated in Section IV. In Section V, an iterative heuristic algorithm is proposed to solve the formulated problem. The performance of the proposed algorithm, substantiated by extensive simulations, is evaluated in Section VI. Concluding remarks are presented in Section VII.

III. SYSTEM MODEL

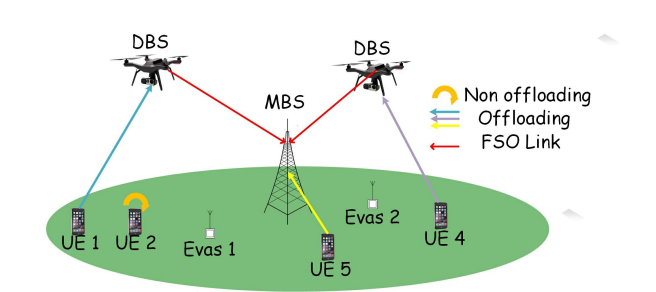


Fig. 1. FSO-enabled DBS-assisted secure MEC network

The FSO-enabled DBS-assisted secure MEC network is proposed to provision ground UEs with the secured fast uplink transmission and computing capabilities. Denote \mathcal{I} , \mathcal{I} , and \mathcal{K} as the set of UEs, base stations (BSs), and eavesdroppers (EVs). As shown in Fig. 1, the MEC network system is composed of $|\mathcal{I}|$ BSs (including an MBS and $(|\mathcal{I}|-1)$ DBSs), $|\mathcal{I}|$ ground UEs and $|\mathcal{K}|$ EVs. We assume the locations and the number of the UEs are known by the MBS and DBS. The number of eavesdroppers is also known by the MBS and DBSs. The locations of the eavesdroppers are imperfectly estimated. Both MBS and DBSs are equipped with multi-core servers, which can handle multiple tasks simultaneously. The server on the MBS is much more powerful than that on the DBS. The UEs

can offload their tasks to either MBS or DBS. Besides serving as computing nodes, DBSs can also work as relays to forward the tasks from UEs to the MBS through the FSO backhaul link. The DBS hovers at a fixed height and UEs are assumed to exhibit low mobility.

A. Communications Model

The communications channel between the *i*-th user equipment UE_i and the *j*-th DBS DBS_j is assumed to be probabilistic LoS [9] expressed as:

$$p_{ij}^{los} = \frac{1}{1 + ae^{-b(\theta_{ij} - a)}}, j > 1,$$
 (1)

where a and b are environmental parameters corresponding to different terrains, e.g., urban or rural [18]. $\theta_{ij} = \arctan(h_j/l_{ij})$ denotes the elevation angle between UE_i and DBS_j . Here, l_{ij} and h_j are the horizontal and vertical distance between UE_i and the DBS_j , respectively.

The LoS and non-LoS path loss between UE_i and DBS_j (j = 1 represents the MBS) are respectively expressed as:

$$\varphi_{ij}^{los} = \zeta^{los} + \tau^{los} \log_{10}(\sqrt{l_{ij}^2 + h_j^2}), j > 1,$$
 (2)

$$\varphi_{ij}^{nlos} = \zeta^{nlos} + \tau^{nlos} \log_{10}(\sqrt{l_{ij}^2 + h_j^2}), j > 1,$$
 (3)

where τ^{los} and τ^{nlos} are the LoS and non-LoS path exponent, respectively. ζ^{los} and ζ^{nlos} are the LoS and non-LoS path loss at a reference distance, respectively [19], [20]. Thus, we can derive the average path loss from UE_i to DBS_i as:

$$\varphi_{ij} = p_{ij}^{los} \varphi_{ij}^{los} + (1 - p_{ij}^{los}) \varphi_{ij}^{nlos}, j > 1.$$
 (4)

Here, $p_{ij}^{nlos} = 1 - p_{ij}^{los}$ is the probability of non-LoS connection between UE_i and DBS_j .

The UE is associating with the MBS if j = 1. The path loss between the UE_i and the MBS is expressed as:

$$\varphi_{ij} = \zeta^m + \tau^m \log_{10}(\sqrt{l_{ij}^2 + h_j^2}), j = 1.$$
 (5)

Here, ζ^m is the path loss at the reference distance and τ^m the path exponent from UE_i to the MBS. Thus, we can derive the data rate from UE_i to BS_i :

$$R_{ij} = b_{ij} \log_2(1 + \frac{p_i 10^{\frac{-\varphi_{ij}}{10}}}{\sigma^2}), \tag{6}$$

where b_{ij} is the bandwidth allocated to UE_i by BS_j . p_i is the transmission power of UE_i and σ^2 is the noise power. The path loss between UE_i and the k-th eavesdropper (EV_k) can be written as [13]:

$$\varphi_{ik}^{e} = \zeta^{e} + \tau^{e} \log_{10}(l_{ik}^{e}), \tag{7}$$

where ζ^e and τ^e are the path loss at the reference distance and path exponent between UE_i and EV_k , respectively. l_{ik}^e is the distance between UE_i and EV_k . Then, we can derive the data rate between UE_i and EV_k as:

$$R_{ik}^{e} = \sum_{i=1}^{|\mathcal{F}|} b_{ij} \log_2(1 + \frac{p_i 10^{\frac{-\varphi_{ik}^{e}}{10}}}{\sigma^2}).$$
 (8)

To secure the network, our objective is to minimize the eavesdropper's transmission rate. Also, to minimize the task completion time of UEs, our objective is to maximize the legitimate aggregate transmission rate of the UEs. Since we consider both objectives, the secrecy rate is utilized to quantify the security level of the network, which is defined as the data rate between the UE and base station minus the data rate between the eavesdropper and UE. The secrecy rate R_{ij}^s of UE_i when associating with BS_j is given by [21]:

$$R_{ij}^{s} = \left[R_{ij} - \max_{k \in \mathcal{K}} \{R_{ik}^{e}\}\right]^{+}, \forall i \in \Omega \cup \Psi.$$
 (9)

Here, $[x]^+ \triangleq \max\{0, x\}$. Ω is the set of the UEs who offload their tasks directly to BS_j . Ψ is the set of the UEs who offload their tasks to MBS through the relay of DBS_j (j > 1).

The FSO link channel gain between the MBS and DBS_j is given by [22]:

$$h_i^{FSO} = e^{-\beta L_j}, j > 1,$$
 (10)

where L_j is the distance from DBS_j to MBS. The atmospheric attenuation coefficient β is calculated by:

$$\beta = \frac{3.91}{V} (\frac{\lambda}{550})^{-q},\tag{11}$$

where λ is the wavelength of the FSO link. V is the maximum distance the laser beam can travel. q is the size distribution of the scattering particles given by [23]:

$$q = \begin{cases} 0 & V \le 0.5, \\ V - 0.5 & 0.5 < V \le 1, \\ 0.16V + 0.34 & 1 < V \le 6, \\ 1.3 & 6 < V \le 50, \\ 1.6 & 50 < V, \end{cases}$$
(12)

where V depends on the weather conditions such as: V > 50 when the weather is clear and V < 1 when it is foggy. The data rate of the FSO link between DBS_j and MBS can be calculated as:

$$R_j^{FSO} = \frac{p_j^{FSO}}{E_p N_b} \frac{r_s^2}{(\theta_g L_i)^2} \eta_t \eta_r 10^{-h_j^{FSO}}, j > 1.$$
 (13)

Here, p_j^{FSO} is the transmission power of DBS_j . E_p is the photon energy calculated by $E_p = Hc/\lambda$, where H and c are the Planck's constant and the light speed, respectively. N_b is the sensitivity of the FSO receiver (photons/bit). r_s is the radius of the FSO receiver at the MBS. θ_g is the divergence angle of the laser beam. η_t and η_r are the transmitter and receiver efficiency, respectively.

B. Computing Model

All the BSs (including the MBS and DBSs) are equipped with multi-core servers to provide computing services. The server mounted on the MBS is assumed to be more powerful than those mounted on the DBSs. Because the size of the computation result is often considerably much smaller than the size of uploaded data, the transmission latency for BS_j to send the result back to UE_i is neglected in general [24], [25]. Denote d_i as the task size of UE_i . The task completion time for UE_i to offload the task to BS_j equals to:

$$t_{ij}^{b} = \frac{d_i}{R_{ij}} + \frac{r_i d_i}{C_{ij}},\tag{14}$$

where r_i is the required computing resource per bit and C_{ij} is the computing resources allocated to UE_i by BS_j .

The completion time for the task forwarded to the MBS by DBS_j consists of the transmission time from UE_i to DBS_j , transmission time from DBS_j to MBS, and the computing time, which can be expressed as:

$$t_{ij}^{f} = \frac{d_i}{R_{ij}} + \frac{d_i}{R_i^{FSO}} + \frac{r_i d_i}{C_{ij}}, j > 1.$$
 (15)

The task completion time for local execution can be expressed as:

$$t_i^l = \frac{r_i d_i}{C_i^l},\tag{16}$$

where C_i^l is the computing capacity of UE_i .

The power consumption of the task initialized by UE_i for the remote computing p_{ij}^r and the local computing p_i^l can be calculated by [26]:

$$p_{ij}^r = \kappa_j^r C_{ij}^3, \forall i \in \mathcal{I}, \forall j \in \mathcal{J},$$
(17)

$$p_i^l = \kappa_i^l(C_i^l)^3, \forall i \in \mathcal{I}, \tag{18}$$

where κ_j^r and κ_i^l are the computing power coefficient of the BS_i and UE_i , respectively.

Let $\alpha_i \in \{0,1\}$ indicate whether UE_i processes the task locally $(\alpha_i = 1)$ or remotely $(\alpha_i = 0)$. $\omega_{ij} \in \{0,1\}$ indicates whether the task initialized by UE_i is offloaded to BS_j $(\omega_{ij} = 1)$ or not $(\omega_{ij} = 0)$. $\psi_{ij} \in \{0,1\}$ indicates whether the task initialized by UE_i is relayed to the MBS through DBS_j $(\psi_{ij} = 1)$ or not $(\psi_{ij} = 0)$. Thus, we can derive the task completion time of UE_i as:

$$T_{ij} = T_i^l + T_{ij}^b + T_{ij}^f, (19)$$

where $T_i^l = \alpha_i (1 - \omega_{ij}) (1 - \psi_{ij}) t_i^l$ is the local computing time, $T_{ij}^b = \omega_{ij} (1 - \alpha_i) (1 - \psi_{ij}) t_{ij}^b$ is the task completion time if UE_i offloads the task to BS_j , and $T_{ij}^f = \psi_{ij} (1 - \alpha_i) (1 - \omega_{ij}) t_{ij}^f$ is the task completion time if UE_i offloads its task to the MBS through the relay of DBS_j . We assume one task can only be processed locally or remotely, and the task can only be executed by one entity. Thus, the constraint $\alpha_i + \sum_{j=1}^{|\mathcal{J}|} \omega_{ij} + \sum_{i=1}^{|\mathcal{J}|} \psi_{ij} = 1, \forall i \in \mathcal{J}$ must be satisfied.

TABLE 1. List of Key Notations

$\mathcal{I},\mathcal{J},\mathcal{K}$	Set of UEs, BSs, EVs
Ω, Ψ	Set of offloading UEs with and without relay
R_{ij}^s	Secrecy rate between UE_i and BS_j
$R_{ij}^{s,lb}$	Lower bound of the secrecy rate between UE_i and BS_j
$R_{ik}^{e,ub}$	Upper bound of the data rate between UE_i and EV_k
Γ_{ij}	Distance between UE_i and BS_j
$\widetilde{R}_{ij}^{(1)}$	First-order Taylor expansion of $R_{ij}^{s,lb}$ w.r.t. p_i
$\widetilde{T}_{ij}^{(1)}$	First-order Taylor expansion of T_{ij} w.r.t. p_i
$\widetilde{R}_{ij}^{(2)}$	First-order Taylor expansion of $R_{ij}^{s,lb}$ w.r.t. Γ_{ij}
$\widetilde{T}_{ij}^{(2)}$	First-order Taylor expansion of T_{ij} w.r.t. Γ_{ij}
$\widetilde{T}_{ij}^{(3)}$	First-order Taylor expansion of T_{ij} w.r.t. A

IV. PROBLEM FORMULATION

The objective of this article is to maximize the average secrecy rate of all offloading UEs and minimize the average task completion time of all the tasks. We define $Z \triangleq \{(x_j, y_j), \forall j \in \mathcal{J}, j > 1\}$ as the set of locations of DBSs. $P^{DBS} \triangleq \{p_j^{FSO}, \forall j \in \mathcal{J}, j > 1\}$ as the DBS transmission power. $P^{UE} \triangleq \{p_i, \forall i \in \mathcal{J}\}$ as the UE transmission power. $F \triangleq \{C_{ij}, \forall i \in \mathcal{F}, \forall j \in \mathcal{J}\}$ as the BS computing resource allocation. $A \triangleq \{\alpha_i, \omega_{ij}, \psi_{ij}, \forall i \in \mathcal{F}, \forall j \in \mathcal{J}\}$ as the UE association. $B \triangleq \{b_{ij}, \forall i \in \mathcal{F}, \forall j \in \mathcal{J}\}$ as the bandwidth allocation. Thus, we formulate the following multi-objective optimization problem to solve the TENSOR problem:

$$\mathcal{P}_{1}: \max_{Z,P^{DBS},P^{UE},F,B,A} \sum_{i \in \Omega \cup \Psi} \sum_{j \in \mathcal{J}} \frac{1}{|\Omega| + |\Psi|} R_{ij}^{s}$$

$$\min_{Z,P^{DBS},P^{UE},F,B,A} \sum_{i \in \mathcal{J}} \sum_{j \in \mathcal{J}} \frac{1}{|\mathcal{J}|} T_{ij}$$

$$s.t.: C1: \sum_{i=1}^{|\mathcal{J}|} \omega_{ij} C_{ij} + \sum_{i=1}^{|\mathcal{J}|} \psi_{ij} C_{ij} \leq C_{j}^{Dmax}, \forall j \in \mathcal{J}$$

$$C2: \sum_{i=1}^{|\mathcal{J}|} \omega_{ij} b_{ij} + \sum_{i=1}^{|\mathcal{J}|} \psi_{ij} b_{ij} \leq B_{j}^{Dmax}, \forall j \in \mathcal{J}$$

$$C3: P_{j}^{FSO} + \sum_{i=1}^{|\mathcal{J}|} \omega_{ij} p_{i}^{r} \leq P_{j}^{Dmax}, \forall j \in \mathcal{J}, j > 1$$

$$C4: \alpha_{i} + \sum_{j=1}^{|\mathcal{J}|} \omega_{ij} + \sum_{j=1}^{|\mathcal{J}|} \psi_{ij} = 1, \forall i \in \mathcal{J}$$

$$C5: (1 - \alpha_{i}) p_{i} + \alpha_{i} p_{i}^{l} \leq P_{i}^{Umax}, \forall i \in \mathcal{J}$$

$$C6: \sum_{j=1}^{|\mathcal{J}|} T_{ij} \leq T_{i}^{DL}, \forall i \in \mathcal{J}$$

$$C7: 0 \leq x_{j}, y_{j} \leq 500, \forall j \in \mathcal{J}$$

$$C8: \alpha_{i} = \{0, 1\}, \forall i \in \mathcal{J}, \forall j \in \mathcal{J}$$

$$C9: \omega_{ij} = \{0, 1\}, \forall i \in \mathcal{J}, \forall j \in \mathcal{J}$$

$$C10: \psi_{ij} = \{0, 1\}, \forall i \in \mathcal{J}, \forall j \in \mathcal{J}$$

Here, C_j^{Dmax} , B_j^{Dmax} , and P_j^{Dmax} are the maximum computing, bandwidth, and power capacities of BS_j . P_i^{Umax} is the power capacity of UE_i , respectively. T_i^{DL} is the deadline of the task initialized by UE_i . C1 and C2 are computing resource and bandwidth capacity constraints, which impose the computing resource and bandwidth allocated to UE not to exceed the capacity of the BS. C3 is the DBS power capacity which imposes the power used for FSO communication and computing not to exceed the capacity of the DBS. C4 is the UE association constraint which imposes one task to only be processed by one device. C5 is the UE power constraint which imposes the power used for computing and the communication not to exceed the device capacity. C6 is the task deadline constraint which imposes the task completion time not to exceed the deadline of the task. C7 is the DBS placement constraint on the horizontal plane. C8-C10 are the binary constraints.

V. PROPOSED SOLUTION

The TENSOR problem is a mixed-integer nonlinear problem due to the UE association indicators, and the data rate function being neither convex nor concave w.r.t. the placement of the DBS; it is thus very challenge to solve TENSOR. Furthermore, the uncertainty of the eavesdropper's location has exacerbated the difficulty of TENSOR. To tackle the problem, we adopt the bounded location error model to describe the eavesdroppers' uncertainty given by [27]:

$$z_k \in \{||z_k - \bar{z}_k|| \le \delta\},\tag{21}$$

where z_k is the location of EV_k . \bar{z}_k is the estimated location of EV_k by BSs. δ is the estimation error. The physical meaning of this model is that the location of EV_k can be anywhere within the cycle with radius δ and center at \bar{z}_k . Since this model is still an uncertainty model, to solve the problem, we consider the location of EV_k that results in the worst-case lower bound of the secrecy rate:

$$R_{ij}^{s,lb} = [R_{ij} - \max_{k \in \mathcal{K}} \{R_{ik}^{e,ub}\}]^+, \forall i \in \Omega \cup \Psi,$$
 (22)

where $R_{ik}^{e,ub} = b_{ij} \log_2(1 + \frac{p_i 10^{-\frac{\varphi_i^{s,lb}}{10}}}{\sigma^2})$ is the upper bound of the data rate between the UE_i and EV_k . Here, $\varphi_{ik}^{s,lb} =$ $\zeta_{ik}^e + \tau_{ik}^e \log_{10}(\sqrt{||z_i - \bar{z}_k|| - \delta})$ and z_i denotes the location of UE_i . Then, we can restate \mathcal{P}_1 as:

$$\mathcal{P}'_{1} : \max_{Z,P^{DBS},P^{UE},F,B,A} \sum_{i \in \Omega \cup \Psi} \sum_{j \in \mathcal{J}} \frac{1}{|\Omega| + |\Psi|} R^{s,lb}_{ij}$$

$$\min_{Z,P^{DBS},P^{UE},F,B,A} \sum_{i \in \mathcal{J}} \sum_{j \in \mathcal{J}} \frac{1}{|\mathcal{J}|} T_{ij}$$

$$s.t. : C1 - C10 \tag{23}$$

Due to the binary indicators and the secrecy rate function, \mathcal{P}'_1 is a mixed-integer nonlinear problem. Moreover, \mathcal{P}'_1 is not convex due to the DBS placement. To solve the multiobjective problem, we utilize the ϵ -constraint method, which is to put one of our objectives into the constraint. Here, we put the second objective into the constraint because the second objective is to minimize the average task completion and we can easily find the upper bound of the objective, which is $\epsilon = \sum_{i=1}^{|\mathcal{I}|} \frac{1}{|\mathcal{I}|} T_i^{DL}$. Then, we restate \mathscr{P}'_1 as:

$$\mathcal{P}_{2}: \max_{Z,P^{DBS},P^{UE},F,B,A} \sum_{i \in \Omega \cup \Psi} \sum_{j \in \mathcal{J}} \frac{1}{|\Omega| + |\Psi|} R_{ij}^{s,lb}$$

$$s.t.: C1 - C10$$

$$C11: \sum_{i=1}^{|\mathcal{J}|} \sum_{j=1}^{|\mathcal{J}|} \frac{1}{|\mathcal{J}|} T_{ij} \le \epsilon$$
(24)

After implementing the ϵ -constraint method, \mathcal{P}_2 is still a mixed-integer nonlinear problem and not convex, due to the binary indicators, secrecy rate function, and DBSs placement. In order to solve \mathcal{P}_2 , we decompose \mathcal{P}_2 into 4 sub-problems: bandwidth and computing resource allocation problem, UE power control problem, DBSs placement problem, and UE association problem. Then, we use successive convex approximation to tackle the problem.

A. The Bandwidth and Computing Resource Allocation Prob-

For given UE transmission power, DBSs placement, and UE association, \mathcal{P}_2 can be simplified to \mathcal{P}_{2-A} :

$$\mathcal{P}_{2-A} : \max_{B,F} \sum_{i \in \Omega \cup \Psi} \sum_{j \in \mathcal{J}} \frac{1}{|\Omega| + |\Psi|} R_{ij}^{s,lb}$$

$$s.t. : C1, C2, C3, C6, C11$$
(25)

Note that C3 imposes the power used for FSO communication and computing not to exceed the capacity of the DBS. To minimize the task completion time, the equality condition of C3 will always hold. As a result, we can conclude that $P_i^{FSO} =$ $P_j^{Dmax} - \sum_{i=1}^{|\mathcal{J}|} \omega_{ij} p_i^r$. By substituting P_j^{FSO} in Eq. (13), we decide P^{DBS} in \mathcal{P}_2 .

Lemma 1. Given UE transmission power, DBSs placement, and UE association, \mathcal{P}_{2-A} is convex.

Proof: We can derive the Hessian Matrix of $R_{ij}^{s,lb}$ as $H^{R} = \begin{bmatrix} \frac{\partial^{2} R_{ij}^{s,lb}}{\partial^{2} b_{ij}} & \frac{\partial^{2} R_{ij}^{s,lb}}{\partial b_{ij} \partial C_{ij}} \\ \frac{\partial^{2} R_{ij}^{s,lb}}{\partial C_{ij} \partial b_{ij}} & \frac{\partial^{2} R_{ij}^{s,lb}}{\partial^{2} C_{ij}} \end{bmatrix} = \begin{bmatrix} 0 & 0 \\ 0 & 0 \end{bmatrix}, \text{ i.e., } H^{R} \text{ is both}$

positive and negative semi-definite, which is linear w.r.t b_{ij} and C_{ij} . As a result, $R_{ij}^{s,lb}$ is convex. Since the linear combination of convex functions is still convex, we can conclude that the objective function of \mathcal{P}_{2-A} is convex. For constraints C1, C2, and C3, they are obviously convex (linear). For constraints C6 and C11, denote the Hessian

Matrix of
$$T_{ij}$$
 as $H^T = \begin{bmatrix} \frac{\partial^2 T_{ij}}{\partial^2 b_{ij}} & \frac{\partial^2 T_{ij}}{\partial b_{ij} \partial C_{ij}} \\ \frac{\partial^2 T_{ij}}{\partial C_{ij} \partial b_{ij}} & \frac{\partial^2 T_{ij}}{\partial^2 C_{ij}} \end{bmatrix}$. There are two cases based on different UE association policy. $H^T = \begin{bmatrix} 0 & 0 & 1 \end{bmatrix}$

two cases based on different OE association pointy.
$$H = \begin{bmatrix} 0 & 0 \\ 0 & 0 \end{bmatrix}$$
 (obviously convex), if task i is executed locally.
$$H^{T} = \begin{bmatrix} \frac{2d_{i}M}{b_{ij}^{3}log(1+\gamma_{i})} & 0 \\ 0 & M(\frac{2r_{i}d_{i}}{C_{ij}^{3}} + \frac{2d_{i}(\kappa_{j}^{r})^{2}}{N(P_{j}^{Dmax} - C_{ij}\kappa_{j}^{r})^{3}}) \end{bmatrix}, \text{ if task}$$

i is executed by BS *j*. Here, $\gamma_i = \frac{p_i 10^{-\frac{\varphi_{ij}}{10}}}{\sigma^2}$, $M = \omega_{ij} (1 - \omega_{ij})$ $\alpha_i)(1-\psi_{ij})+\psi_{ij}(1-\alpha_i)(1-\omega_{ij})$ and $N=\frac{r_s^2\eta_t\eta_r10^{-h_f^{FSO}}}{E_pN_b(\theta_gL_j)^2}$. Since the task is executed remotely (i.e., M=1), we have $P_i^{Dmax} - C_{ij}\kappa_i^r \geq 0$. This is because the power used for computing will never exceed the power capacity of the DBS. $N, \kappa_i^r, r_i, d_i, b_{ij}$ and C_{ij} are all larger than 0. As a result, H^T is positive semi-definite, implying that T_i is convex for a given UE association. Since the summation of convex functions is still convex, we can conclude that \mathcal{P}_{2-A} is convex.

Since \mathcal{P}_{2-A} is convex, we can solve it easily by CVX.

B. The UE Transmission Power Problem

For given bandwidth and computing resource allocation, DBSs placement, and UE association, \mathcal{P}_2 can be simplified to \mathcal{P}_{2-B} :

$$\mathcal{P}_{2-B} : \max_{P^{UE}} \sum_{i \in \Omega \cup \Psi} \sum_{j \in \mathcal{J}} \frac{1}{|\Omega| + |\Psi|} R_{ij}^{s,lb}$$

$$s.t. : C5, C6, C11$$
(26)

However, the objective function $R_{ij}^{s,lb} = [R_{ij} - R_{ik}^{e,ub}]^+$ is not convex w.r.t. the UE transmission power p_i . Although R_{ij} and $R_{ik}^{e,ub}$ are both convex w.r.t. p_i , the subtraction of R_{ij} and $R_{ik}^{e,ub}$ is not necessarily convex. To convexify \mathcal{P}_{2-B} , we try to replace R_{ij} and $R_{ij}^{e,ub}$ with their first-order Taylor expansion. Denote $\widetilde{R}_{ij}^{(1)}$ as the first-order Taylor expansion of $R_{ij}^{s,lb}$ w.r.t. p_i , then,

$$\begin{split} \widetilde{R}_{ij}^{(1)} &= b_{ij} \log(1 + \frac{p_i[m]10^{-\frac{\varphi_{ij}}{10}}}{\sigma^2}) - b_{ij} \log(1 + \frac{p_i[m]10^{-\frac{\varphi_{ij}}{10}}}{\sigma^2}) + (\frac{b_{ij}10^{-\frac{\varphi_{ij}}{10}}}{\sigma^2 \log(1 + \frac{p_i[m]10^{-\frac{\varphi_{ij}}{10}}}{\sigma^2})} + \frac{b_{ij}10^{-\frac{\varphi_{ik}^e}{10}}}{\sigma^2})(p_i - p_i[m]), \end{split}$$

$$\frac{\sigma^2 \log(1 + \frac{p_i[m]10^{-\frac{\varphi_{ik}^e}{10}}}{\sigma^2})(p_i - p_i[m]), \tag{27}$$

where $p_i[m]$ is the transmission power of UE_i at the m-th iteration. Then, we define the first-order Taylor expansion of T_{ij} w.r.t. p_i as $\widetilde{T}_{ij}^{(1)}$, which can be expressed as:

$$\widetilde{T}_{ij}^{(1)} = (T_i^l)^{(1)} + (T_{ij}^b)^{(1)} + (T_{ij}^f)^{(1)}, \tag{28}$$

where $(T_i^l)^{(1)}=\alpha_i(1-\omega_{ij})(1-\psi_{ij})\frac{r_id_i}{C_i^{IE}}$ is the first-order Taylor expansion of T_i^l . $(T_{ij}^b)^{(1)}=\omega_{ij}(1-\alpha_i)(1-\psi_{ij})(b_{ij}\log_2(1+\frac{p_i[m]10^{-\frac{\varphi_{ij}}{10}}}{\sigma^2})+\frac{r_id_i}{C_{ij}}-\frac{d_i10^{-\frac{\varphi_{ij}}{10}}}{\sigma^2b_{ij}\log_2(1+\frac{p_i[m]10^{-\frac{\varphi_{ij}}{10}}}{\sigma^2})^2(1+\frac{p_i[m]10^{-\frac{\varphi_{ij}}{10}}}{\sigma^2})}$ $p_i[m]))$ is the first-order Taylor expansion of T_{ij}^b w.r.t. p_i . $(T_{ij}^f)^{(1)}=\psi_{ij}(1-\alpha_i)(1-\omega_{ij})(\frac{(T_{ij}^b)^{(1)}}{\omega_{ij}(1-\alpha_i)(1-\psi_{ij})}+\frac{d_i}{R_j^{FSO}})$ is the first-order Taylor expansion of T_{ij}^f w.r.t. p_i . At last, we restate \mathcal{P}_{2-B} as:

$$\mathcal{P}'_{2-B} : \max_{P^{UE}} \sum_{i \in \Omega \cup \Psi} \sum_{j \in \mathcal{J}} \frac{1}{|\Omega| + |\Psi|} \widetilde{R}_{ij}^{(1)}$$

$$s.t. : C5$$

$$C6' : \sum_{j=1}^{|\mathcal{J}|} \widetilde{T}_{ij}^{(1)} \le T_i^{DL}, \forall i \in \mathcal{J}$$

$$C11' : \sum_{i=1}^{|\mathcal{J}|} \sum_{j=1}^{|\mathcal{J}|} \frac{1}{|\mathcal{J}|} \widetilde{T}_{ij}^{(1)} \le \epsilon$$

$$(29)$$

Since $\widetilde{R}_{ij}^{(1)}$ and $\widetilde{T}_{ij}^{(1)}$ are linear (i.e., convex) functions of p_i , \mathscr{P}_{2-B}' is a convex problem, which can be solved by utilizing CVX.

C. The DBS Placement Problem

For given UE transmission power, DBS transmission power, BS computing resource allocation, bandwidth allocation and UE association, \mathcal{P}_2 can be simplified to \mathcal{P}_{2-C} :

$$\mathcal{P}_{2-C} : \max_{Z} \sum_{i \in \Omega \cup \Psi} \sum_{j \in \mathcal{J}} \frac{1}{|\Omega| + |\Psi|} R_{ij}^{s,lb}$$

$$s.t. : C6, C7, C11$$

$$(30)$$

Note that \mathscr{P}_{2-C} is neither convex nor concave w.r.t. the location of DBS_j , (x_j, y_j) , since R_{ij} is neither convex nor concave w.r.t. (x_j, y_j) . However, R_{ij} and T_{ij} is convex and concave w.r.t. Γ_{ij} , respectively, where $\Gamma_{ij} = \sqrt{l_{ij}^2 + h_j^2}$ is the distance between UE_i and DBS_j . To solve the DBS placement problem, we try to transform \mathscr{P}_{2-C} into a convex problem by replacing R_{ij} and T_{ij} with their convex approximations. Define $\widetilde{R}_{ij}^{(2)}$ as the first-order Taylor expansion of $R_{ij}^{s,lb}$ w.r.t. Γ_{ij} and define $\widetilde{T}_{ij}^{(2)}$ as the first-order Taylor expansion of T_{ij} w.r.t. Γ_{ij} . Then, we can restate \mathscr{P}_{2-C} as:

$$\mathcal{P}'_{2-C} : \max_{\Gamma_{ij}} \sum_{i \in \Omega \cup \Psi} \sum_{j \in \mathcal{J}} \frac{1}{|\Omega| + |\Psi|} \widetilde{R}_{ij}^{(2)}$$

$$s.t. : C6'' : \sum_{j=1}^{|\mathcal{J}|} \widetilde{T}_{ij}^{(2)} \le T_i^{DL}, \forall i \in \mathcal{J}$$

$$C7' : \Gamma_{ij} \in [h, \sqrt{h^2 + (500\sqrt{2})^2}]$$

$$C11'' : \sum_{i=1}^{|\mathcal{J}|} \sum_{j=1}^{|\mathcal{J}|} \frac{1}{|\mathcal{J}|} \widetilde{T}_{ij}^{(2)} \le \epsilon$$
(31)

Here, C7' is the distance constraint. The smallest and largest value of Γ_{ij} are obtained when DBS_j is right above UE_i and when DBS_j and UE_i are at two diagonal corners, respectively. Since \mathcal{S}'_{2-C} is convex, we can solve it by utilizing CVX.

D. UE Association Problem

For given UE transmission power, DBS transmission power, BS computing resource allocation, bandwidth allocation and DBS placement, \mathcal{P}_2 can be simplified to \mathcal{P}_{2-D} :

$$\mathcal{P}_{2-D} : \max_{A} \sum_{i \in \Omega \cup \Psi} \sum_{j \in \mathcal{J}} \frac{1}{|\Omega| + |\Psi|} R_{ij}^{s,lb}$$

$$s.t. : C1 - C6, C8 - C11$$
(32)

Note that \mathcal{P}_{2-D} is a multiple-choice multiple-dimension knapsack problem, which is a well-known NP-hard problem. To solve the problem, we first rewrite the binary constraints C8 - C10 as follows:

$$C8': 0 \leq \alpha_{i} \leq 1, \forall i \in \mathcal{F}$$

$$C8'': \sum_{i=1}^{|\mathcal{F}|} \alpha_{i} - \alpha_{i}^{2} \leq 0$$

$$C9': 0 \leq \omega_{ij} \leq 1, \forall i \in \mathcal{F}, \forall j \in \mathcal{F}$$

$$C9'': \sum_{i=1}^{|\mathcal{F}|} \sum_{j=1}^{|\mathcal{F}|} \omega_{ij} - \omega_{ij}^{2} \leq 0$$

$$C10': 0 \leq \psi_{ij} \leq 1, \forall i \in \mathcal{F}, \forall j \in \mathcal{F}$$

$$C10'': \sum_{i=1}^{|\mathcal{F}|} \sum_{j=1}^{|\mathcal{F}|} \psi_{ij} - \psi_{ij}^{2} \leq 0$$
(33)

Then, we restate \mathcal{P}_{2-D} as:

$$\mathcal{P}'_{2-D} : \min_{A} L(A, \eta_{\alpha}, \eta_{\omega}, \eta_{k}) \triangleq \sum_{i \in \Omega \cup \Psi} \sum_{j \in \mathcal{J}} \frac{-1}{|\Omega| + |\Psi|} R_{ij}^{s,lb} +$$

$$\eta_{\alpha} (\sum_{i=1}^{|\mathcal{J}|} \alpha_{i} - \alpha_{i}^{2}) + \eta_{\omega} (\sum_{i=1}^{|\mathcal{J}|} \sum_{j=1}^{|\mathcal{J}|} \omega_{ij} - \omega_{ij}^{2})$$

$$+ \eta_{k} (\sum_{i=1}^{|\mathcal{J}|} \sum_{j=1}^{|\mathcal{J}|} \psi_{ij} - \psi_{ij}^{2})$$

$$s.t. : C1 - C6, C8', C9', C10', C11$$
(34)

Here, η_{α} , η_{ω} , and η_{k} are the penalty factors that penalize the UE association indicators that violate constraints C8'', C9'', and C10''.

Lemma 2. For sufficiently large penalty factors η_{α} , η_{ω} , and η_k , \mathcal{P}'_{2-D} is equivalent to \mathcal{P}_{2-D} .

Proof: We can observe that $\max_{A} \sum_{i \in \Omega \cup \Psi} \sum_{j \in \mathcal{J}} \frac{1}{|\Omega| + |\Psi|} R_{ij}^{s,lb}$ in \mathcal{P}_{2-D} is equivalent to $\min_{A} \sum_{i \in \Omega \cup \Psi} \sum_{j \in \mathcal{J}} \frac{1}{|\Omega| + |\Psi|} R_{ij}^{s,lb}$ in $\mathcal{P}_{2-D}^{\prime}$. Denote the primal solution of $\mathcal{P}_{2-D}^{\prime}$ as $p^* = \min_{A} \max_{\eta_{\alpha},\eta_{\omega},\eta_{k}} L(A,\eta_{\alpha},\eta_{\omega},\eta_{k})$ and the solution of the dual problem as $d^* = \max_{\eta_{\alpha},\eta_{\omega},\eta_{k}} \min_{A} L(A,\eta_{\alpha},\eta_{\omega},\eta_{k})$. According to Lagrangian duality, we have $d^* \leq p^*$. If $\eta_{\alpha}(\sum_{i=1}^{|\mathcal{J}|} \alpha_{i} - \alpha_{i}^{2}) = 0$, $\eta_{\omega}(\sum_{i=1}^{|\mathcal{J}|} \sum_{j=1}^{|\mathcal{J}|} \omega_{ij} - \omega_{ij}^{2}) = 0$, and $\eta_{k}(\sum_{i=1}^{|\mathcal{J}|} \sum_{j=1}^{|\mathcal{J}|} \psi_{ij} - \psi_{ij}^{2}) = 0$, we have $L(A,\eta_{\alpha},\eta_{\omega},\eta_{k}) = \max_{\eta_{\alpha},\eta_{\omega},\eta_{k}} L(A,\eta_{\alpha},\eta_{\omega},\eta_{k})$. Note that $\max_{\eta_{\alpha},\eta_{\omega},\eta_{k}} \min_{A} L(A,\eta_{\alpha},\eta_{\omega},\eta_{k}) \geq \min_{A} L(A,\eta_{\alpha},\eta_{\omega},\eta_{k})$. Thus, we can conclude that $d^* = p^*$. Since $\min_{A} L(A,\eta_{\alpha},\eta_{\omega},\eta_{k})$ is increasing monotonically w.r.t. η_{α} , η_{ω} , and η_{k} , we can conclude that $p^* = \min_{A} L(A,\eta_{\alpha},\eta_{\omega},\eta_{k})$. If $\eta_{\alpha}(\sum_{i=1}^{|\mathcal{J}|} \sum_{j=1}^{|\mathcal{J}|} \psi_{ij} - \psi_{ij}^{2}) > 0$, $\max_{\eta_{\alpha},\eta_{\omega},\eta_{k}} \min_{A} L(A,\eta_{\alpha},\eta_{\omega},\eta_{k})$ is increasing monotonically w.r.t. η_{α} , η_{ω} , and η_{k} , which contradicts $d^* \leq p^*$. As a result, for enough large penalty factors, \mathcal{P}_{2-D}' is equivalent to \mathcal{P}_{2-D} .

In the objective function of \mathscr{S}'_{2-D} , $\eta_{\alpha}(\sum_{i=1}^{|\mathcal{F}|} \alpha_i - \alpha_i^2)$, $\eta_{\omega}(\sum_{i=1}^{|\mathcal{F}|} \sum_{j=1}^{|\mathcal{F}|} \omega_{ij} - \omega_{ij}^2)$, and $\eta_k(\sum_{i=1}^{|\mathcal{F}|} \sum_{j=1}^{|\mathcal{F}|} \psi_{ij} - \psi_{ij}^2)$ are all composed by subtracting two convex functions, which are not necessarily convex. So, we construct a surrogate function by implementing the first order Taylor approximation to the objective function of \mathscr{P}'_{2-D} . Define $L'(A, \eta_{\alpha}, \eta_{\omega}, \eta_k)$ as the first order Taylor expansion of the objective function of \mathscr{P}'_{2-D} , $L'(A, \eta_{\alpha}, \eta_{\omega}, \eta_k) \triangleq L(A[m], \eta_{\alpha}, \eta_{\omega}, \eta_k) + \nabla_{\alpha}L(A[m], \eta_{\alpha}, \eta_{\omega}, \eta_k)(\alpha - \alpha[m]) + \nabla_{\omega}L(A[m], \eta_{\alpha}, \eta_{\omega}, \eta_k)$ $(\omega - \omega[m]) + \nabla_k L(A[m], \eta_{\alpha}, \eta_{\omega}, \eta_k)(k - k[m])$. Here A[m], $\alpha[m]$, $\omega[m]$, and k[m] are the UE association at the m-th iteration. Define $T_{ij}^{(3)}$ as the first-order Taylor expansion of T_{ij} w.r.t. A, then $T_{ij}^{(3)}$ can be expressed as:

$$\widetilde{T}_{ii}^{(3)} = (T_i^l)^{(3)} + (T_{ii}^b)^{(3)} + (T_{ii}^f)^{(3)}, \tag{35}$$

where $(T_i^l)^{(3)} = \alpha_i[m](1 - \omega_{ij}[m])(1 - \psi_{ij}[m])t_i^l + (1 - \omega_{ij}[m])(1 - \psi_{ij}[m])t_i^l(\alpha_i - \alpha_i[m])$ is the first-order Taylor expansion of T_i^l . $(T_{ij}^b)^{(3)} = \omega_{ij}[m](1 - \alpha_i[m])(1 - \psi_{ij}[m])t_{ij}^b + (1 - \alpha_i[m])(1 - \psi_{ij}[m])t_{ij}^b(\omega_{ij} - \omega_{ij}[m])$ is the first-order

Taylor expansion of T_{ij}^b . $(T_{ij}^f)^{(3)} = \psi_{ij}[m](1 - \alpha_i[m])(1 - \omega_{ij}[m])T_{ij}^f + (1 - \alpha_i[m])(1 - \omega_{ij}[m])T_{ij}^f(\psi_{ij} - \psi_{ij}[m])$ is the first-order Taylor expansion of T_{ij}^f . Then, we can restate \mathcal{P}'_{2-D} as:

$$\mathcal{P}_{2-D}^{"}: \min_{A} L^{\prime}(A, \eta_{\alpha}, \eta_{\omega}, \eta_{k})$$

$$s.t.: C1 - C5, C8^{\prime}, C9^{\prime}, C10^{\prime}$$

$$C6^{"}: \sum_{j=1}^{|\mathcal{J}|} \widetilde{T}_{ij}^{(3)} \leq T_{i}^{DL}, \forall i \in \mathcal{J}$$

$$C11^{"}: \sum_{i=1}^{|\mathcal{J}|} \sum_{j=1}^{|\mathcal{J}|} \frac{1}{|\mathcal{J}|} \widetilde{T}_{ij}^{(3)} \leq \epsilon$$

$$(36)$$

Since \mathcal{P}''_{2-D} is convex, we can solve it by using CVX.

E. Proposed Algorithm

Algorithm 1: Iterative Allocation for TENSOR

Input: $I, D, E, C_j^{Dmax}, P_j^{Dmax}, B_j^{Dmax}, P_i^{Umax}, T_i^{DL}$. **Output:** $F, B, P^{DBS}, P^{UE}, A, Z$.

- 1 Initialize m and set m = 1.
- 2 Initialize $P^{UE}[m]$, $P^{DBS}[m]$, A[m], and Z[m].
- 3 repeat
- 4 Given $P^{UE}[m]$, $P^{DBS}[m]$, A[m], and Z[m], obtain F[m+1], B[m+1], and $P^{DBS}[m+1]$ by solving \mathcal{P}_{2-A} .
- 5 Given A[m], Z[m], F[m+1], B[m+1], and $P^{DBS}[m+1]$, obtain $P^{UE}[m+1]$ by solving \mathcal{P}'_{2-B} .
- 6 Given A[m] F[m+1], B[m+1], $P^{DBS}[m+1]$, and $P^{UE}[m+1]$, obtain Z[m+1] by solving \mathcal{P}'_{2-C} .
- 7 Given F[m+1], B[m+1], $P^{DBS}[m+1]$, $P^{UE}[m+1]$, and Z[m+1], obtain A[m+1] by solving \mathcal{P}_{2-D}'' .
- 8 m = m + 1.

9 unti

$$\sum_{i \in \Omega[m+1] \cup \Psi[m+1]} \sum_{j \in \mathcal{J}} \frac{1}{|\Omega[m+1] + |\Psi[m+1]|} R_{ij}^{s,lb} [m+1] - \sum_{i \in \Omega[m] \cup \Psi[m]} \sum_{j \in \mathcal{J}} \frac{1}{|\Omega[m] + |\Psi[m]|} R_{ij}^{s,lb} [m] \le \varepsilon.$$

Based on the analysis in the proposed solution section, our proposed iterative algorithm is illustrated in Algorithm 1. We iteratively slove \mathcal{P}_{2-A} , \mathcal{P}'_{2-B} , \mathcal{P}'_{2-C} , and \mathcal{P}''_{2-D} (Steps 3-8) until the improvement of the average secrecy rate (Step 9) is less than the threshold ε .

Lemma 3. Algorithm 1 is guaranteed to converge.

Proof: Denote $R^{s,lb}(\cdot)$ as the objective function of TENSOR. $F[m], B[m], P^{DBS}[m], P^{UE}[m], A[m],$ and Z[m] are the BS computing resource allocation, BS bandwidth assignment, FSO transmission power, UE transmission power, and DBS placement at the m-th iteration, respectively. In Algorithm 1 line 4, since \mathscr{P}_{2-A} is convex w.r.t. F, B, and $P^{DBS}, R^{s,lb}(F[m+1], B[m+1], P^{DBS}[m+1], P^{UE}[m], A[m], Z[m]) ≥ <math>R^{s,lb}(F[m], B[m], P^{DBS}[m], P^{UE}[m], P^{UE}[m], A[m], Z[m])$. In line 5, we set the output of \mathscr{P}_{2-A} (e.g., F[m+1], B[m+1],

and $P^{DBS}[m+1]$) as the input of \mathcal{P}'_{2-B} . Since \mathcal{P}'_{2-B} is convex w.r.t. P^{UE} , $R^{s,lb}(F[m+1], B[m+1], P^{DBS}[m+1])$ 1], $P^{UE}[m+1]$, A[m], Z[m]) $\geq R^{s,lb}(F[m+1], B[m+1])$ 1], $P^{DBS}[m + 1]$, $P^{UE}[m]$, $P^{DBS}[m]$, A[m], Z[m]). line 6, we set the output of \mathcal{P}_{2-A} and \mathcal{P}'_{2-B} (e.g., $F[m+1], B[m+1], P^{DBS}[m+1]$, and $P^{UE}[m+1]$) as the input of \mathscr{P}'_{2-C} . Since \mathscr{P}'_{2-C} is convex w.r.t. Z, $R^{s,lb}(F[m+1], B[m+1], P^{DBS}[m+1], P^{UE}[m+1], A[m], Z[m+1]) <math>\geq R^{s,lb}(F[m+1], A[m], Z[m+1]) \geq R^{s,lb}(F[m+1], Z[m+1$ 1], B[m+1], $P^{DBS}[m+1]$, $P^{UE}[m+1]$, A[m], Z[m]). In line 7, we set the output of \mathcal{P}_{2-A} , \mathcal{P}'_{2-B} , and \mathcal{P}'_{2-C} (e.g., F[m+1], B[m+1], $P^{DBS}[m+1]$, $P^{UE}[m+1]$, and Z[m+1]) as the input of \mathcal{P}''_{2-D} . Since \mathcal{P}''_{2-D} is convex w.r.t. A, $R^{s,lb}(F[m+1],B[m+1],P^{DBS}[m+1],P^{UE}[m+1],A[m+1])$ 1], Z[m + 1]) $\geq R^{s,lb}(F[m + 1], B[m + 1], P^{DBS}[m + 1])$ 1], $P^{UE}[m+1]$, A[m], Z[m+1]). So, $R^{s,lb}(F[m+1], B[m+1])$ 1], $P^{DBS}[m+1]$, $P^{UE}[m+1]$, A[m+1], Z[m+1]) \geq $R^{s,lb}(F[m], B[m], P^{DBS}[m], P^{UE}[m], A[m], Z[m]),$ which indicates that Algorithm 1 yields a non-decreasing sequence of the objective value. The upper bound of $R^{s,lb}$ is reached when there is no eavesdropper, i.e., $R^{s,lb} = \sum_{i \in \Omega \cup \Psi} \sum_{j \in \mathcal{J}} \frac{1}{|\Omega| + |\Psi|} R_{ij}$. Hence, we conclude that Algorithm 1 is guaranteed to converge.

VI. PERFORMANCE EVALUATION

Extensive simulations are run using MATLAB to obtain the results. In the simulations, UEs and EVs are uniformly distributed in a $500\times500~m^2$ area. The MBS is placed in the center of the area. The two DBSs are also initially placed in the center of the area. We assume one raspberry pi 4 is mounted on each DBS. Since each CPU core of the raspberry pi 4 can overclock to 2.3 GHz [28], the computational capacity of the DBS is $4\times2.3=9.2$ GHz (four cores). According to [29], the specific absorption rate for mobile devices is 1.6 W/Kg and the weight of smart phones range from 112 g to 328 g. Therefore, the transmission power of each UE is randomly distributed within [100,500] mW. The task size and the deadline of each task are distributed within [0.1,0.5] Mb and [0.2,1] s, respectively [30]. The other simulation parameters are illustrated in Table 2.

Fig. 2 shows how the average secrecy rate of offloaded UEs changes for different numbers of UEs. There are 2 EVs and 3 BSs in Fig. 2. The yellow bar corresponds to 4 UEs, the pink bar 8 UEs, the cyan bar 12 UEs, the red bar 16 UE, and the green bar 20 UEs. Note that the average secrecy rate increases as the number of UEs increases from 4 to 12 (yellow to cyan bar) because the DBSs have enough resource to serve UEs. However, from 12 to 20 UEs (cyan to green bar) the average secrecy rate decreases as the number of UEs increases because the DBSs do not have enough resources to serve all UEs, i.e., some UEs have to offload their tasks to the MBS. Since the channel capacity of the MBS is smaller than that of the eavesdropper unless the UE is very close to the MBS, connecting to the MBS will cause information leakage. As a result, the secrecy rate of some UEs may reduce drastically. Thus, as the number of UEs grows, more UEs will have zero secrecy rate, thus resulting in the decrease of the average secrecy rate. The result shows that, when the number of UEs

TABLE 2. Simulation Parameters

(a, b) environmental parameters	(9.1,0.16) [33]
$(\xi_{ij}^{los}, \xi_{ij}^{nlos}, \tau_{ij}^{los}, \tau_{ij}^{nlos})$	(1,20,20,20) [9] [36]
(ξ_{ij}^m, au_{ij}^m)	(131.1,42.8) [10]
(ξ_{ik}, au_{ik})	(80,20) [34]
σ^2	-174 dbm/Hz
$(B_1^{Dmax}, B_j^{Dmax}, \forall j > 1)$	(20, 5) MHz [10] [35]
$(C_1^{Dmax}, C_j^{Dmax}, \forall j > 1)$	(50, 9.2) GHz [32] [28]
p_i	[100, 500] mW [28] [29]
r_i	$[0.2, 1] \times 10^5$ cycles/bit [30]
d_i	[0.1, 0.5] Mb [30]
T_i^{DL}	[0.2, 1] s [30]
h_j	25 m
$P_j^{Dmax}, \forall j > 1$	3.5 W [28]
N_b	100 photons/bit [31]
r_s	0.05 m [31]
$ heta_{\mathcal{g}}$	1 mrad [31]
λ	1550 nm [31]
V	10 km [31]
(X_{max}, Y_{max})	(500, 500) m

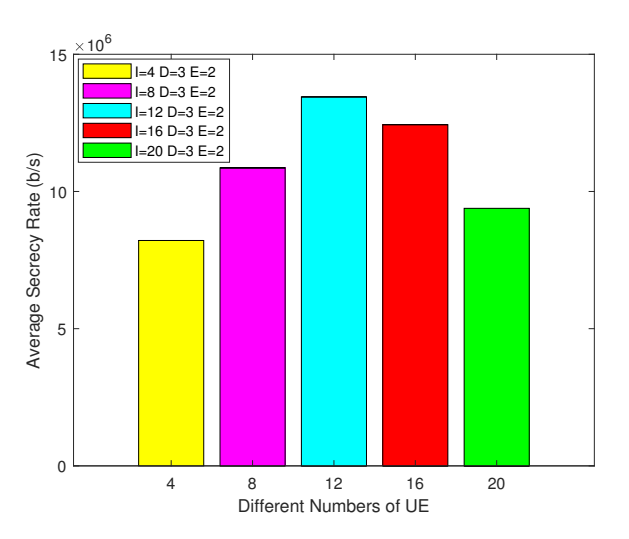


Fig. 2. Average secrecy rate for different numbers of UE.

is over 12, in order to increase the secrecy rate, we should deploy more DBSs.

Fig. 3 demonstrates how the average secrecy rate changes as the number of EVs increases. In Fig. 3, there are 4 UEs and 3 BSs. The yellow, pink, cyan and red bar correspond to 1, 2, 3, and 4 EVs, respectively. The result shows that the average secrecy rate decreases as the number of EVs increases. This is quite intuitive, with the increase of EVs, the possibility of EVs being closer to UEs will also increase. Therefore, UEs will face more threats as the number of EVs increases.

Fig. 4 illustrates the average secrecy rate for different ϵ . In Fig. 4, there are 8 UEs, 3 BSs, and 2 EVs. $\epsilon = \sum_{i=1}^{|\mathcal{J}|} \frac{1}{I} T_i^{DL}$, which is the average deadline of all the tasks corresponding to the constraint C11 of \mathcal{P}_2 . The value of the x-axis in Fig. 4 reflects a multiplier of ϵ , i.e., 0.7 means 0.7ϵ . The results show that the average secrecy rate decreases as ϵ decreases. As the task deadline constraint becomes stricter, the DBSs

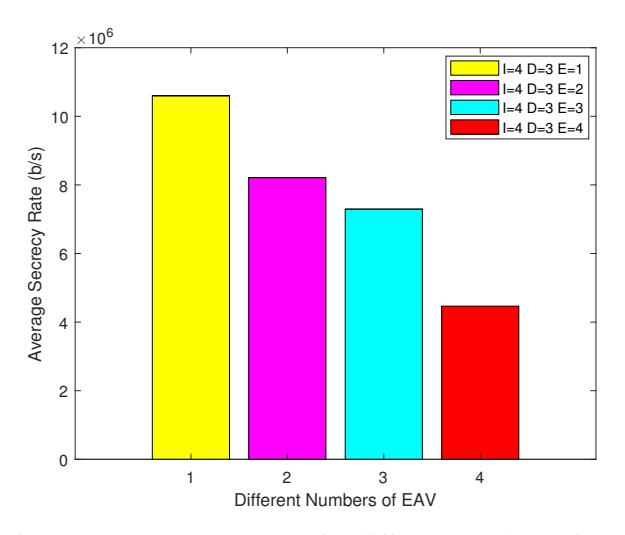


Fig. 3. Average secrecy rate for different numbers of EAV.

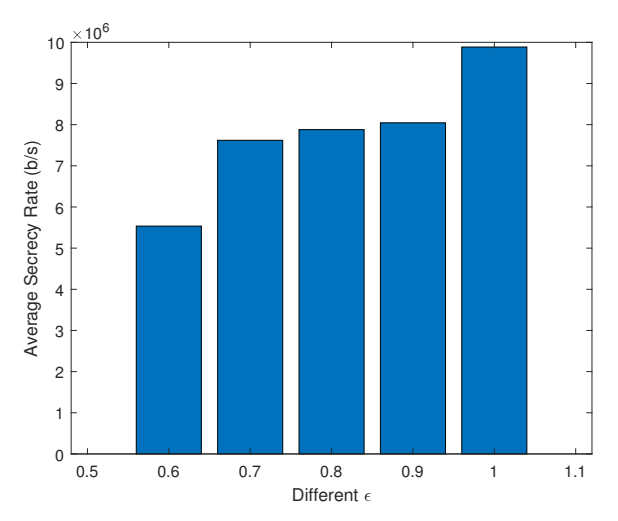


Fig. 4. Average secrecy rate for different ϵ .

have to fly closer to the UEs which have a larger task size, and allocate more resources to them. Since DBSs do not have enough resources, more UEs have to offload their tasks to the MBS, thus decreasing the average secrecy rate. In addition, when the task deadline constraint is smaller than 0.6ϵ there will be no solution, i.e., when the task deadline constraint is smaller than 0.6ϵ , more DBSs are needed.

Fig. 5 illustrates the average secrecy rate for different algorithms. In Fig. 5, "E" is the abbreviation for equal share resource allocation, "G" represents the greedy algorithm. "F" stands for fix placement, and "M" stands for the block searching placement method. There are 12 UEs, 3 BS, and 2 EVs. RF stands for the fixed placement random algorithm where the DBSs are placed in the center of the area and UEs have the same probabilities to offload their tasks to any BSs. The resources are allocated to UEs to meet the deadline requirements. EF represents the fixed placement equal allocation algorithm, in which the DBSs are fixed in the center of the area and the resources are equally shared by all the UEs. Meanwhile, UEs transmit at their maximum power. GM

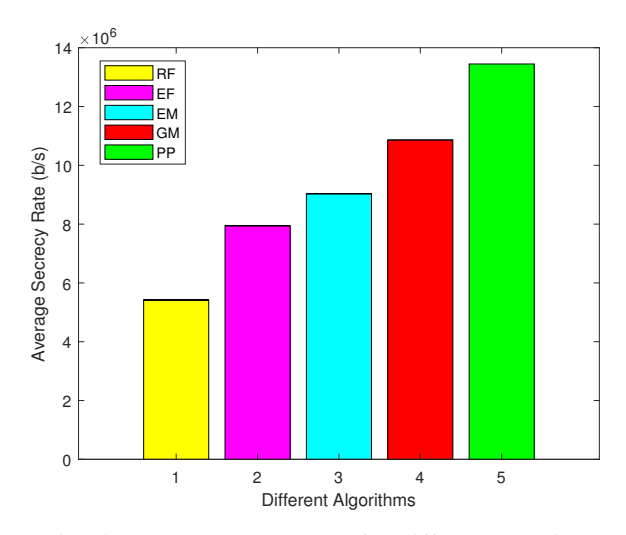


Fig. 5. Average secrecy rate for different algorithm.

and EM algorithms share the same placement policy in which the plane is divided into multiple blocks, and the DBSs search every block to find a place that maximizes the average secrecy rate. The difference between the GM and EM algorithms is the UE association policy. For the GM algorithm, UEs are sorted in descending order according to d_i/T_i^{DL} and have the same probability to offload their tasks to any DBSs. The tasks are first offloaded to the DBSs with the sorted order until all resources are exhausted. Then, all the remaining tasks will be offloaded to the MBS. For the EM algorithm, UEs share all the available resources equally and have the same probability to offload their tasks to any BSs. PP is our proposed algorithm. The result shows that our proposed algorithm is better than the other four algorithms. For the GM algorithm, UEs offload their tasks to the DBSs blindly with equal probability. However, UEs may not choose the most suitable DBS that incurs the highest secrecy rate. For instance, the tasks that are offloaded to DBS₁ may yield higher secrecy rates if they are offloaded to DBS_2 . Also, the same situation may happen for tasks that are offloaded to DBS2. The reason why EM is inferior to GM is that all UEs in GM try to offload their tasks to DBSs. Different from the GM algorithm, all UEs have the same probability to offload their tasks to the MBS and DBSs in the EM algorithm. A UE associated with DBSs will increase the secrecy rate as compared to associating with the MBS. The performance of our proposed algorithm is improved by 19% as compared to the GM algorithm when there are 12 UEs and 2 EVs.

VII. CONCLUSION

In this article, we have formulated the TENSOR problem in which an MBS and multiple DBSs are deployed to provide computing services to the ground UEs. FSO is implemented to provide high-speed backhaul. The objective is to jointly maximize the average secrecy rate of all offloading UEs and minimize the average task completion time of all UEs. In order to solve TENSOR, a successive convex approximation technique has been applied. Specifically, we have decomposed TENSOR into four sub-problems: resource assignment and

DBS transmission power control problem, UE power control problem, UE association problem, and DBS placement problem. Then, these four sub-problems are cyclically optimized in each iteration, i.e., the output of the first three as the input for the fourth. However, the UE power control problem, UE association problem, and DBS placement problem are not convex. Thus, we convexify these three sub-problems by leveraging the Taylor approximation and solving them approximately. A cyclic iterative algorithm, which is guaranteed to converge, has been designed. The simulation results demonstrate that our proposed algorithm achieves better performance as compared to the greedy allocation algorithm, equal allocation algorithm, random association algorithm, and block search placement.

REFERENCES

- [1] M. A. Hossain and N. Ansari, "Energy Aware Latency Minimization for Network Slicing Enabled Edge Computing," *IEEE Trans. Green Commun. Netw.*, vol. 5, no. 4, pp. 2150-2159, Dec. 2021.
- [2] N. M. Karie, N. M. Sahri and P. Haskell-Dowland, "IoT Threat Detection Advances, Challenges and Future Directions," 2020 Workshop on Emerging Technologies for Security in IoT (ETSecIoT), 2020, pp. 22-29.
- [3] D. G. Chandra and M. D. Borah, "Cost Benefit Analysis of Cloud Computing in Education," 2012 International Conference on Computing, Communication and Applications, 2012, pp. 1-6.
- [4] W. Liu, L. Zhang and N. Ansari, "Laser Charging Enabled DBS Placement for Downlink Communications," *IEEE Trans. Netw. Sci. Eng.*, vol. 8, no. 4, pp. 3009-3018, Oct.-Dec. 2021.
- [5] A. R. Hossain and N. Ansari, "Priority-Based Downlink Wireless Resource Provisioning for Radio Access Network Slicing," *IEEE Trans. Veh. Technol.*, vol. 70, no. 9, pp. 9273-9281, Sept. 2021.
- [6] A. Majumdar, "Free-Space Laser Communication Performance in the Atmospheric Channel," Springer J. Optical and Fiber Commun. Reports, vol. 2, no. 4, Oct. 2005, pp. 345–96.
- [7] Rizzo, L., Federici, J.F. et al., "Comparison of Terahertz, Microwave, and Laser Power Beaming Under Clear and Adverse Weather Conditions," *Journal of Infrared, Millimeter, and Terahertz Waves*, vol. 41, no. 8, pp. 979–996, Jun. 2020.
- [8] Rizzo, L., Duncan, K.J. et al., "Direct beam hazard analysis of large beam diameters for laser power beaming," *Journal of Laser Applications*, vol. 30, no. 3, 032017, 2018.
- [9] A. Al-Hourani, S. Kandeepan, and S. Lardner, "Optimal LAP altitude for maximum coverage," *IEEE Wireless Commun. Lett.*, vol. 3, no. 6, pp. 569–572, Dec. 2014.
- [10] L. Zhang and N. Ansari, "Latency-Aware IoT Service Provisioning in UAV-Aided Mobile-Edge Computing Networks," *IEEE Internet Things* J., vol. 7, no. 10, pp. 10573-10580, Oct. 2020.
- [11] L. Yang, H. Yao, J. Wang, C. Jiang, A. Benslimane and Y. Liu, "Multi-UAV-Enabled Load-Balance Mobile-Edge Computing for IoT Networks," *IEEE Internet Things J.*, vol. 7, no. 8, pp. 6898-6908, Aug. 2020.
- [12] J. Si, Z. Cheng, Z. Li, J. Cheng, H. -M. Wang and N. Al-Dhahir, "Cooperative Jamming for Secure Transmission With Both Active and Passive Eavesdroppers," *IEEE Trans. Commun.*, vol. 68, no. 9, pp. 5764-5777, Sept. 2020.
- [13] J. Yao and N. Ansari, "Secure Federated Learning by Power Control for Internet of Drones," *IEEE Trans. Cogn. Commun. Netw.*, vol. 7, no.4, pp. 1021-1031, Dec. 2021.
- [14] J. C. Liu, J. Lee and T. Q. S. Quek, "Safeguarding UAV Communications Against Full-Duplex Active Eavesdropper," *IEEE Trans. Wireless Commun.*, vol. 18, no. 6, pp. 2919-2931, June 2019.
- [15] N. Zhao et al., "Caching UAV Assisted Secure Transmission in Hyper-Dense Networks Based on Interference Alignment," *IEEE Trans. Commun.*, vol. 66, no. 5, pp. 2281-2294, May 2018.
- [16] F. Cheng et al., "UAV-Relaying-Assisted Secure Transmission With Caching," *IEEE Trans. Commun.*, vol. 67, no. 5, pp. 3140-3153, May 2019.
- [17] J. Miao and Z. Zheng, "Cooperative Jamming for Secure UAV-Enabled Mobile Relay System," *IEEE Access*, vol. 8, pp. 48943-48957, 2020.
- [18] M. Alzenad, A. El-Keyi and H. Yanikomeroglu, "3-D Placement of an Unmanned Aerial Vehicle Base Station for Maximum Coverage of Users With Different QoS Requirements," *IEEE Wireless Commun. Lett.*, vol. 7, no. 1, pp. 38-41, Feb. 2018.

- [19] Q. Fan and N. Ansari, "Towards Traffic Load Balancing in Drone-Assisted Communications for IoT," *IEEE Internet Things J.*, vol. 6, no. 2, pp. 3633-3640, April 2019.
- [20] A. Fotouhi, M. Ding, and M. Hassan, "Dynamic base station repositioning to improve performance of drone small cells," in Proc. IEEE GLOBECOM, Dec. 2016, pp. 1–6.
- [21] Y. Zhang, Z. Mou, F. Gao, J. Jiang, R. Ding and Z. Han, "UAV-Enabled Secure Communications by Multi-Agent Deep Reinforcement Learning," *IEEE Trans. Veh. Technol.*, vol. 69, no. 10, pp. 11599-11611, Oct. 2020.
- [22] S. Zhang and N. Ansari, "Latency Aware 3D Placement and User Association in Drone-assisted Heterogeneous Networks with FSO-Based Backhaul," *IEEE Trans. Veh. Technol.*, vol. 70, no. 11, pp. 11991-12000, Nov. 2021.
- [23] I. I. Kim et al., "Comparison of laser beam propagation at 785 nm and 1550 nm in fog and haze for optical wireless communications," SPIE Proc. Opt. Wireless Comm. III, vol. 4214, no. 2,pp. 26–37, 2001.
- [24] X. Hou, Z. Ren, J. Wang, S. Zheng, W. Cheng and H. Zhang, "Distributed Fog Computing for Latency and Reliability Guaranteed Swarm of Drones," *IEEE Access*, vol. 8, pp. 7117-7130, 2020.
- [25] L. Li, X. Zhang, K. Liu, F. Jiang, and J. Peng, "An energy-aware task offloading mechanism in multiuser mobile-edge cloud computing," *Mobile Inf. Syst.*, vol. 2018, Apr. 2018, Art. no. 7646705.
- [26] Y. Wen et al., "Energy-optimal mobile application execution: Taming resource-poor mobile devices with cloud clones," *Proceedings IEEE INFOCOM*, 2021, pp. 2716-2720.
- [27] Y. Zhou et al., "Secure Communications for UAV-Enabled Mobile Edge Computing Systems," *IEEE Trans. Commun.*, vol. 68, no. 1, pp. 376-388, Jan. 2020.
- [28] W. Liu, S. Zhang and N. Ansari, "Joint Laser Charging and DBS Placement for Drone-assisted Edge Computing," *IEEE Trans. Veh. Technol.*, vol. 71, no. 1, pp. 780-789, Jan. 2022.
- [29] Federal Communications Commission, "Cell Phones and Specific Absorption Rate," Jun. 2000. [Online]. Available: https://www.fcc.gov/general/cell-phones-and-specific-absorption-rate
- [30] J. Zhang et al., "Joint Resource Allocation for Latency-Sensitive Services Over Mobile Edge Computing Networks With Caching," *IEEE Internet Things J.*, vol. 6, no. 3, pp. 4283-4294, Jun. 2019.
- [31] D. Wu et al., "An FSO-Based Drone Assisted Mobile Access Network for Emergency Communications," *IEEE Trans. Netw. Sci. Eng.*, vol. 7, no. 3, pp. 1597-1606, 1 July-Sept. 2020.
- [32] J. Zhang et al., "Joint Resource Allocation for Latency-Sensitive Services Over Mobile Edge Computing Networks With Caching," *IEEE Internet Things J.*, vol. 6, no. 3, pp. 4283-4294, Jun. 2019.
- [33] S. Zhang and N. Ansari, "3D Drone Base Station Placement and Resource Allocation With FSO-Based Backhaul in Hotspots," *IEEE Trans. Veh. Technol.*, vol. 69, no. 3, pp. 3322-3329, March 2020.
- [34] H. Lee, S. Eom, J. Park and I. Lee, "UAV-Aided Secure Communications With Cooperative Jamming," *IEEE Trans. Veh. Technol.*, vol. 67, no. 10, pp. 9385-9392, Oct. 2018.
- [35] X. Liu and N. Ansari, "Resource Allocation in UAV-Assisted M2M Communications for Disaster Rescue," *IEEE Wireless Commun. Lett.*, vol. 8, no. 2, pp. 580-583, April 2019.
- [36] M. A. Hossain, A. R. Hossain and N. Ansari, "Numerology-capable UAV-MEC for Future Generation Massive IoT Networks," *IEEE Internet Things J.*, 2022, doi: 10.1109/JIOT.2022.3189945.